75th International Astronautical Congress (IAC), Milan, Italy, 14-18 October 2024.

Analysis of intra-vehicular robotic free-flyers and their manipulation capabilities

Federico Turchetti, **Monica Ekal***, **Neal Y. Lii**, **Maximo A. Roa**

Institute of Robotics and Mechatronics, German Aerospace Center (DLR), Oberpfaffenhofen-Weßling, Germany 82234
* *Corresponding author, monica.ekal@dlr.de*

Abstract

Intra-vehicular free-flyer systems (IVFFS), in addition to being micro-gravity test beds for autonomy algorithms, are also used to develop caretaking and crew-assistance capabilities for future space stations. The International Space Station (ISS) has hosted an assortment of IVFFS since the deployment of NASA's SPHERES in 2006, with JAXA's Int-Ball, DLR-Airbus' CIMON and NASA's Astrobee being the current resident IVFFS. Despite the long history of onboard free-flyers, in-space manipulation with IVFFS has been demonstrated to a limited extent. Manipulation capabilities are crucial for onboard autonomy; IVFFS could help alleviate the duties of the crew by performing maintenance or tending to scientific experiments. This paper presents a review of existing IVFFS while examining their potential to perform intra-vehicular manipulation. This discussion is supported by a simulation study of an intra-vehicular floating-base robotic manipulator. Free-flying robot manipulators are governed by distinct dynamics owing to their mobile base, and advanced motion planning and control algorithms are essential for precise task execution. Accounting for the specific considerations of IVFFs, including mass, size, and a constrained environment, a simulation study of the robot's torque requirements while performing a sample cargo grappling task in free-floating and base-stabilization mode is presented. In drawing platform-independent conclusions from this analysis, this paper aims to highlight the requirements and challenges for future IVFFS to raise their autonomy levels by gaining the capability to perform common intra-vehicular manipulation tasks.
Keywords: Space robotic manipulation, Micro-gravity, Intra-vehicular operations.

1. Introduction

Robotic solutions are being developed to boost space exploration in a number of ways, e.g., to mitigate the problems of accumulating debris through on-orbit servicing and life extension, the use of robot manipulators for latching and docking incoming spacecraft on the International Space Station (ISS), for planetary exploration and resource prospecting. As crewed space missions become longer and more frequent, robotics can also support operations inside crewed spacecraft by carrying out housekeeping tasks such as inspection, maintenance, taking inventory and assisting the crew with documentation. By carrying out simple and repetitive tasks, intra-vehicular robots address the issue of limited crew time and consumables.

Intra-vehicular free-flyer systems or IVFFS are free-flying robots deployed in the interior of orbiting stations with the objective of assisting crew and to develop autonomy capabilities. Their free-flying mode of locomotion enables them to freely navigate to a desired point inside the pressurized module, working alongside crew in a reactive manner. By carrying out care-taking tasks that can be easily automated, these assistant robots would reduce the workload of astronauts. Additionally, autonomous IVFFS would be crucial for the maintenance of future orbiting stations like the planned Lunar Gateway[·], which, in addition to being the first space station in lunar orbit, will be uncrewed for extended periods of time.

According to the Japan Aerospace Exploration Agency (JAXA)'s crew-task analysis [1] of the Japanese Experiment Module (JEM), the activities that take up the most crew time are *sample and equipment swap* (INS/DET), *logistics*, in particular unpacking and stowing cargo, and, *monitoring*. These tasks took up respectively 22%, 10% and 8% of the studied crew time. Since they can be broken down into simple and repetitive actions, these tasks are ripe for automation. Further, this work lists down the following considerations for intra-vehicular helper robots: robust and self charging free-flying robots, robot-friendly internal equipment and stowage, limited payload, speed and power.

For the validation of these concepts, multiple IVFFS have been deployed onboard the ISS. They are used as testbeds for the development and validity of a wide range of autonomy algorithms, including guidance and navigation, formation flight, and proximity operations. IVFFS currently onboard the ISS are Astrobee, Int-Ball2 and CIMON-2. Apart from using cameras and sensors for

[·] https://www.nasa.gov/mission/gateway/

monitoring, documentation and navigation, IVFFS would need to perform operations such as cargo handling and operating experiments. For this, manipulation capabilities are essential for truly autonomous IVFFS. However, the topic of intra-vehicular manipulation using free-flyers has been scarcely explored in literature. In spite of the number of IVFFS on board the ISS, Astrobee is the only current IVFFS with a perching arm. This 2 Degrees of Freedom (DoF) arm was developed for grasping handrails and developing manipulation algorithms. Therefore, limited experimental demonstrations exist; the most recent experiments using Astrobee's perching arm include testing of a gecko adhesive gripper, and hopping maneuvers ([2], [3], [4]).

Note that several demonstrations and research on in-orbit manipulation exists: The Space Shuttle, ISS, and the Chinese Space Station Tiangong have used robotic arms for inspection, assembly, docking and repair. Further, demonstrations of key capabilities for on-orbit proximity services such as autonomous docking with a free-floating satellite and Orbital Replacement Unit (ORU) transfer has been demonstrated in-flight on the ETS-VII and Orbital Express missions [5, 6]. While many of these concepts apply to intra-vehicular manipulation, the environments and scales of the two differ: IVFFs are more agile since they operate in dynamic, constrained environments and are smaller in size. Generally the ratio of manipulator to base mass is larger in intra-vehicular manipulation, meaning that the dynamic effects of the arm movement will be noticed to a much larger extent. Safe cargo maneuvering inside a module demands planning and control approaches that are not only robust to uncertainty and localization faults, but also consider limited workspaces and dynamic obstacles.

The objective of this paper is, therefore, two-fold; we provide background on the IVFFs that have been developed, and analyze the evolution of their capabilities and technical aspects like propulsion, navigation and sensor suite. The second focus is on intra-vehicular manipulation, discussing the challenges of endowing IVFFS with such a capability. A simulation study of a sample cargo grasping scenario is provided to support this analysis, highlighting the dynamic coupling between the manipulator and the robot base, and the torques required for completing the task with payloads of different masses. Therefore the contributions of this work are:

- A survey of past IVFFS and their capabilities
- A simulation study of a sample cargo-transportation scenario by an intra-vehicular free-flying manipulator robot. The payload grasping task is studied in free-floating and base-stabilization mode by analysing the reaction motions of the base and the arm, and the joint and base torques required for payloads of different masses and sizes (inertias), while considering thrust, torque and velocity limits.

The paper is structured as follows: sec. 2 presents past and current IVFFs, separating them into initial assistant robots in sec. 2.1 and recent freeflyers in sec. 2.2. Autonomous IVFFS are listed in sec. 3. Sec. 4 introduces the topic of intravehicular manipulation. Its challenges are discussed, and a simulation study of a free-flyer in-space manipulation scenario is presented. This paper wraps up with a discussion in sec. 4.2, and concludes with sec. 5.

2. Existing IVFFS

The first ideas about assistant robots were developed in the 90s, stemming from the need of reducing the workload of the crew members. Initial applications of intra-vehicular robots were focused on reducing crew workload by automating experiment monitoring and execution. The following section describes the very first robots built for this purpose, followed by free-flyers deployed on-board the ISS as experimental test beds for applications ranging from experiment monitoring to astronaut companions.

2.1 First assistive robots

2.1.1 The Charlotte, the first assistive robot to reduce crew-workload

Following an analysis of data on crew-time gathered from the Space Shuttle, SpaceLab and SpaceHab missions, telerobotics and telepresence were identified as solutions to reduce intra - and extra-vehicular crew workload [8]. McDonnel Douglas Aerospace (MDA) developed the Charlotte robot in 1994 to carry out telescience, i.e., remotely perform experiments and monitor them in a volume separate from the crew through teleoperation or preprogrammed commands. Taking into account that existing systems and interfaces in space were designed to be operated by the crew and the prohibitive costs of making these interfaces accessible to robots, the Charlotte system was built for capabilities such as the operation of switches, knobs and buttons, in addition to exchanging samples and performing video surveys. It was a 6 DoF cable-driven robot, controlled by eight servo-controlled cables. The system also had a 3 DoF end-effector. The system had two integrated CCV cameras that provided a view of the end-effector and the workspace.

The Charlotte robot was tested in-flight aboard the Discovery Shuttle during the STS-63 mission in 1995[†], in

[†] https://www.nasa.gov/wp-content/uploads/2023/05/sts-063-press-kit.pdf?emrc=0c4886

(a) Charlotte robot on Shuttle Discovery (Credit: The U.S. National Archives, 1995)

(b) AERCam Sprint flight demonstration (Credit: NASA, 1997)

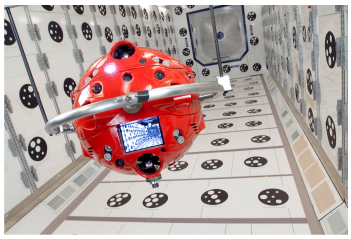

(c) PSA M2B in the ground test facility (Credit: [7], 2006)

Fig. 1. The precursors to intra-vehicular assistive robots

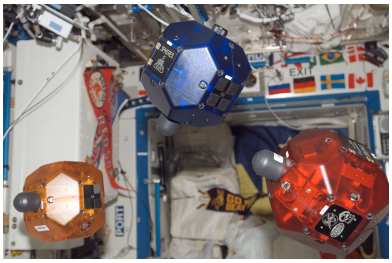

(a) SPHERES onboard the ISS (Credit: NASA, 2006)

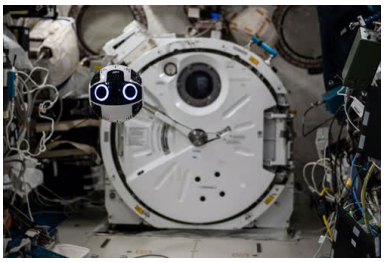

(b) Int-Ball2 onboard the ISS (Credit: JAXA/NASA, 2024)

(c) Astrobee in the ISS JEM (Credit: NASA, 2021)

Fig. 2. IVFFS deployed in space

SpaceHab-3, an on-board, commercially developed pressurized research lab. The test objectives were to demonstrate the system's mobility inside the workspace and its dexterous capabilities, i.e., the control of knobs ans switches on an experiment task panel representative of that used by the crew during experiments.

Following the successful testing of the Charlotte System, the next steps consisted of development of end-effectors that would enable improved remote experiment conduction, and the integration of on-board proximity and collision detection capabilities. The cable-driven nature of the robot afforded precision and coverage of a large workspace, therefore terrestrial applications for this system were envisioned, including aircraft production, maintenance and construction.

2.1.2 AERCam, the first free-flyer in space

While the cable-driven Charlotte robot was the first system designed to reduce crew workload by performing telescience, the Autonomous Extravehicular Activity Robotic Camera Sprint (AERCam Sprint) was the first free-flying robot that was demonstrated in-flight. Sprint was developed with the goal of remote inspection of the spacecraft exterior and viewing of extravehicular activities. Sprint was tested in flight during the 1997 STS-87 mission, by releasing it in the Space Shuttle Orbiter Bay during a spacewalk as well as by remote control via a combination rotational and translational hand controller from insider the Orbiter cockpit [9]. For views of the spacecraft for on-orbit maintenance and servicing, Sprint was equipped with two color video cameras of different focal lengths and a light for illumination.

A second, smaller technology demonstration version of Sprint called Mini AERCam Sprint [10] was developed with reduced mass and size, giving 80% reduction in volume as compared to Sprint. This was achieved by applying miniaturization technology across all subsystems. Lessons learned from Sprint's maiden flight were used in the design of Mini AERCam - it had increased levels of autonomy, was capable of autonomous docking to its docking station, recharging at the parent spacecraft, autonomous station keeping and waypoint tracking [11]. The goal for the Mini was to autonomously carry out external inspections of the spacecraft. Deployment and integration of Mini AERCam for the Space Shuttle and the ISS was proposed, but it was not demonstrated in space.

2.1.3 Personal Satellite Assistant, monitoring and diagnosing free-flyer

NASA's Personal Satellite Assistant (PSA) was a small spherical robot developed to perform mobile-monitoring, communication and diagnosing. It was designed to im-

prove crew productivity by carrying out inventory and payload management, monitoring and task recording, and data display. For this, PSA [12] was equipped with a microphone, a camera and display. Additionally, PSA had an onboard suite of sensors such as pressure, humidity, gas and ambient temperature sensors. These sensors enabled PSA to contribute to spacecraft risk reduction by acting as an element of the spacecraft integrated health management system. PSA could thus help in fault detection by, for instance, generating acoustic, temperature and gas concentration maps, and locating gas and fluid leaks. Multiple prototypes of PSA have been developed over the years. M2B from 2006 was the functional prototype that was developed and fully tested [7]. PSA was tested on ground, including at NASA's 6 DoF Microgravity Test Facility (MGTF), but was not tested in flight.

2.2 Recent Intravehicular free-flyers

2.2.1 CIMON, the AI-based astronaut companion

Working in confined and extreme environments such as those created during long duration space missions poses a risk to overall crew performance and well-being [13]. Designed for reducing crew workload and emotional stress, CIMON (Crew Interactive MObile companioN)[‡], is a technology demonstrator for an AI-based astronaut assistant, developed by Airbus and IBM with funding from the German Aerospace Center (DLR). CIMON is developed with the goal of documentation and assisting the crew with experimental procedures. CIMON acts as a database, a computer and a camera: it can show the required equipment for a task on its screen, present directions for conducting experiments, search for objects and take inventory. Based on the analysis of micro-gravity experiments with CIMON in 2018 and 2019, CIMON-2, an advanced version was launched to the ISS in 2020. CIMON-2 comes with multiple improvements as compared to its predecessor, related to microphone sensitivity, AI capabilities, software stability and 30% increase in autonomy with an advanced sense of orientation[†].

2.2.2 Int-Ball, an on-board autonomous camera

In 2017, Int-Ball [14], a free-flying autonomous camera was developed by JAXA and deployed on-board the ISS. Studies conducted by JAXA showed that crew spends about 10% of their time in documentation via photography and video, and the goal of Int-Ball is to reduce that time to zero. Int-Ball could hold its pose and navigate to a certain point in the JEM under commands from the ground. It had a HD main monitor camera with continuous shooting capabilities. It was capable of target tracking and image stabilization. Based on the results achieved with Int-Ball, the next generation Int-Ball2 [15] was developed, and launched in June 2023. Some key upgrades include improved propulsion, using feature-based navigation instead of target marker, and a docking station for autonomous charging.

2.2.3 SPHERES formation flying testbed

Following in the steps of AERCam and PSA, the Synchronized Position Hold Engage and Reorient Experimental Satellites (SPHERES) were three devices developed by MIT's Space Systems Laboratory, and launched to the ISS in 2006 [16]. The SPHERES platform was envisioned as a long term formation-flying testbed in microgravity to validate high-risk autonomy technologies, in particular, attitude control and station-keeping, collision avoidance, and docking control, without being restricted to 3D and without the time-limit that constrains parabolic flights. SPHERES was the first platform that offered regular sessions for the validation of guest scientist algorithms, outside of MIT, NASA, or the U.S. Department of Defense [17]. SPHERES could be used in three operational environments, including software simulation, a 2D ground laboratory and a 3D ISS laboratory. SPHERES was a hugely successful and long-serving microgravity platform, hosting experiments on formation flights, autonomous docking [18], fluid sloshing [19] and electromagnetic power transfer [20], among others.

2.2.4 Astrobee

Astrobee is NASA's [21] most recent and advanced free-flyer that replaced SPHERES as the space-station's microgravity test facility. Built upon technologies and lessons learned from previous NASA free-flyers, the Astrobee testbed consists of three free-flying robots, whose goal is to provide flight and payload controllers with a mobile camera platform for tasks such as documentation and taking inventory. The future goal for robots such as Astrobee is for them to serve as autonomous caretakers of future spacecraft, performing inspection, maintenance and payload transportation. Additionally, Astrobee is the first free-flyer to have a 2 DoF perching arm. Experiments encompassing varied domains have been carried out using Astrobee, some of them include autonomous logistics management [22], rendezvous with a tumbling object[23], hopping maneuvers using its perching arm [3] and maneuvering in the presence of inertial uncertainty [24]. Further details of some of these IVFFS can be found in Table 1, photos in fig. 2.

[‡] https://www.dlr.de/en/latest/news/2018/1/20180302_cimon-the-intelligent-astronaut-assistant_26307

[†] https://www.airbus.com/en/newsroom/press-releases/2020-04-cimon-2-makes-its-successful-debut-on-the-iss

	PSA (M2B prototype)	*SPHERES*	*Int-Ball2*	*CIMON-2*	*Astrobee*
Organization	NASA	MIT/NASA	JAXA	Airbus/DLR	NASA
Purpose	Crew-assistance, Monitoring	Formation-flying testbed	Documentation	AI-based crew assistant	HW and SW Test facility
Launch year	N/A	2006	2023	2019	2019
Mass	1 Kg	4 Kg	3.3 Kg	5 Kg	6 Kg
Size	ϕ: 15 cm	$21 \times 21 \times 21$ cm	ϕ: 20 cm	ϕ: 32 cm	$32 \times 32 \times 32$ cm
Manipulator	N/A	N/A	N/A	N/A	2 DoF arm
Navigation system	Fiducial markers	Transmission based	Feature-based	Feature-based	Feature-based
Sensors	Stereo cameras Proximity sensors Accelerometers	23 Ultrasonic sensors 5 Ultrasonic beacons Inertial sensors	3 Ultrasonic sensors Navigation camera 7 MEMS inertial sensors Docking I/F	Ultrasonic sensors IR camera Front camera Side camera 3D Camera Inertial sensors 7 Microphones	Navigation camera 3D Hazard camera Science camera Speed camera Inertial sensors Dock camera Perch camera
Display	LCD screen Laser pointer LED spotlight	-	LED lights around “eyes”	LCD screen	Crew touch screen
Propulsion	2 Blowers 4 Reaction wheels	12 Thrusters (CO_2) Tank life 90 min	8 Axial fans	12 air propellers	2 Impellers and 12 vents Perching arm
Batteries	Consummable NiMH battery pack	Rechargeable 13 AA Alkaline batteries	Autonomous recharge	Rechargeable	Autonomous recharge
Battery life	N/A	2h	2h	>2h	3 - 9h
Experiments	N/A	Docking Sloshing Gripper Electromagnetic formation flight Machine Learning	N/A	N/A	Hopping Formation flight Logistics Gripper

Table 1. A comparison of some recent intra-vehicular free-flyers and their capabilities. For IVFFS where a second version was launched to the ISS, the new version is listed

In addition to the free-flyers mentioned above, some others have been proposed in literature. In [25], a small robot capable of grasping small objects, pushing buttons or twisting switches called the Space Humming Bird (SHB) was presented. It has a variable structured body, consisting of two softballs with a stereocamera mounted on its 'head'. The manipulator hand is placed at the beak location, which can be extended to the desired length to grip an object or carry out tasks. Free-flying prolonged-contact manipulations are not possible; a suction disk is mounted on the tail to fix it to any flat surface for the robot to carry out manipulation operations. In [26], an holonomic, intra-vehicular six rotor aerial robot called Space Cobot is presented. Potential collaborative applications for the Space CoBot are telepresence, tracking and manipulation of small free-flying objects such as screws and pens, termed as debris scavenging, and astronaut stabilization, where the robot uses its propulsion to control the velocity of an astronaut who begins to drift away while performing a manual task. The robot is propelled by a hexarotor arrangement with non-parallel axes, that enables holonomic motion and maximum thrust across all directions.

3. Technical aspects

The following section describes specific technical aspects of IVFFs. We do not study the cable-driven Charlotte robotic system and AERCam Sprint in detail, focusing specifically on robot free-flyers that have been deployed inside pressurized modules in space. However, flight experiments with the Charlotte robotic system (1995) and AERCam Sprint (1997) yielded key insights regarding capabilities desired from these robots, in particular autonomous maneuvering, obstacle detection and avoidance, improved vision and improved localization using absolute sensors [27] [‡].

3.1 Navigation

Self-stabilization, accurate relative localization and autonomous maneuvering to a desired point within the workspace are crucial for autonomous intra-vehicular operations. Generally, on-board sensors in the Inertial Measurement Unit (IMU) such as gyroscopes and accelerometers provide high-frequency odometry data. Optical flow measurements are also used for visual odometry. This estimate is error-prone due to sensor noise bias and cumulative errors. Therefore, data from visual sensors about the robot's position in a fixed reference frame of the environment is fused with inertial data in the pose estimation procedure using sensor fusion and filtering approaches. Transmitter-based localization approaches (ultrasonic, infrared or radio-frequency) were prevalent in the early 2000's, however, this requires the addition of transmitters in the operational volume. Vision-based localization can be separated into two categories: the reliance on fiducial markers placed in the environment, and non-fiducial localization that use features intrinsic to the environment. Each category has its drawbacks: the former requires installation of markers in the experiment module, while feature-based navigation on the ISS is a challenge due to the uniform, cluttered, dynamic environment and varying lighting conditions.

Owing to the then-low TRLs of the feature-based navigation, the 2006 model of the PSA used circular fiducial markers. The markers featured 6 white circles on a black one (these can be seen in fig.1c). This was not considered ideal due to the requirement of adding multiple markers in the ISS volume (results from using 302 markers are presented in [7]), and a move to feature-based navigation was planned. An Extended Kalman Filter (EKF) was used to fuse vision and inertial sensor data into a single estimates.

Similar to PSA, the first version of the Int-ball performed vision-based navigation via two stereoscopic markers installed on the airlock and portside of the JEM, using its image navigation camera. A fusion of camera information, IMU and three units of ultrasonic distance sensors are used for estimating the robot's pose within the JEMs coordinate system. The requirement that the markers be in the robot's field of view at all times was seen as limiting. Therefore, the newer version of the Int-Ball, Int-Ball2 adopts visual-based SLAM (Simultaneous Localization and Mapping), using its stereocamera to acquire features from the environment.

The SPHERES navigation system used ultrasonic time-of-flight measurements, i.e., the time taken for the signal emitted by transmitters at known locations within the experimental volume to reach the ultrasonic microphones on the surface of the SPHERES satellites. These measurements arrived at a frequency of 1-2 Hz. The time-of-flight measurements were converted to ranges for position and attitude determination. The satellites, however, needed to turn off their thrusters to listen to the ultrasonic pulses. The SPHERES navigation and localization framework, called Position and Attitude Determination System (PADS) calculated state information at 50 Hz, via a Kalman Filter fusion of information from the global and the local (IMU) navigation results. [16]

CIMON uses vision-based navigation, i.e., a dual 3D camera to collect depth information and relation between features to build a map relying on SLAM algorithms. Additionally, it has directional microphones to orient itself to the speaker, and then use its front camera to establish and

[‡] https://ntrs.nasa.gov/api/citations/20120002583/downloads/20120002583.pdf

maintain eye contact[§].

Astrobee uses images of the module interior from its monocular RGB camera, and compares detected features with those of an on-board map. The fusion of inertial data with feature-based matching gives pose estimates, with the use of visual odometry for short distances where no features from the map are recognized [21]. Given the sensitivity of the original localization approach to environmental factors and occlusions from cargo bags, Astrobee's new localization algorithm, AstroLoc uses a graph-based visual-inertial localization approach that improves pose and IMU bias estimation accuracy and is robust to outliers and Visual odometry faults. [28].

3.1.1 Safety and Obstacle detection

Space Stations are a dynamic environment consisting of cables, laptops and cargo, and IVFFS have to work in close proximity to crew and other IVFFS. Safety is therefore a key factor dictating IVFFS design. All of the existing free-flyers are designed to either be circular (PSA, Intball, CIMON) or with blunt edges to minimize the impact of collision (SPHERES and Astrobee). Additionally, they are lightweight and slow-moving, for instance, Astrobee's maximum speed is 0.5m/s with limited thrust capabilities. Fans and propellers are embedded inside the robot and covered for additional safety when being handled by the crew, e.g., Int-Ball. Ultrasound sensors are commonly used for obstacle detection, with this approach being used in the PSA [7] and CIMON[¶]. Int-ball also has ultrasonic distance sensors used for localization, but its means of obstacle detection is not explicitly stated. Instead the Int-Ball relies on the monitoring of large impulse forces for collision detection and triggers quick responses to it. Astrobee's HazCam is a depth sensor that uses LIDAR to detect obstacles [21].

3.2 Propulsion

The propulsion for IVFFS relies on compressed gas, either using gas tanks or air inside the ISS module, to generate thrust. This air is then expelled through thrusters placed on the robot body. In general, twelve thrusters are used for complete 6 DoF motion through the module.

Like the AERCam Sprint, which was designed to operate outside the spacecraft and used nitrogen as propellant, the SPHERES were the only other gas-propelled free-flyers. The SPHERES used tanks filled with pressurized CO2 in liquid form which lasted for about 10 mins, to be replaced by the crew when empty. Its twelve thrusters have a maximum capacity of 0.2N [16], and as mentioned earlier, had to be shut off to allow for the ultrasound localization pulses to be heard.

During the development of the PSA, the option of cold-gas thrusters was discarded for safety reasons. Six pairs of back-to-back placed ducted fans were used, with translation achieved by symmetric, linear thrusting of pairs and rotation by differential thrusting. PSA's fans provide a linear thrusting capacity of 0.5N [7]. Astrobee uses a fan layout conceptually similar to PSA, where the air pressurized by two large impellers on Astrobee's body is precisely released through twelve vents on its surface. A maximum thrust of 0.6N is achieved on at least one axis. [29].

Int-Ball had 12 micro axial fans for holding a certain pose, and was the only free-flyer to use reaction wheels for attitude stabilization [14]. Each propeller had a maximum thrust capacity of about 1mN, which posed a challenge to maintain hovering, as the robot was swept away in areas of heavy air-flow inside the ISS. Based on the lessons learnt from the Int-Ball, Int-Ball2 now uses 8 large propeller modules, allowing for larger thrust per propeller. It can now produce about 0.15 N on the dominant X axis [15]. The Int-Ball2 system does not have reaction wheels.

CIMON has 14 internal fans that allow independent control in all six DoF [30]. This changed for CIMON-2, which has 12 internal fans[¨]. CIMON's thrust is limited between 0.03 to 0.12 N across the three axes for safety.

3.3 Power

Evidently all free-flyers are battery operated. During the AERCam, PSA and SPHERES projects, the need for having rechargeable batteries rather than consumables was highlighted. Subsequent free-flyers, i.e., Int-Ball and Astrobee were powered using rechargeable batteries. Int-Ball2 and Astrobee also have an autonomous docking capability where the robots use their cameras and the markers on the docking station (AR markers for IntBall and fiduciary markers for Astrobee) for precise docking [31, 32].

3.4 On-board computing

While the avionics and software architecture of each of these IVFFS are different, certain commonalities can be observed. Computationally-intensive modules, in particular, the vision loop are off-boarded to a separate processor or core within the same processor. Time-critical and high-frequency modules like propulsion are naturally given the highest priority. Owing to the evolution of micro-processors and increase in free-flyer computing demands, a shift is also observed in the type of proces-

[§] https://connectorsupplier.com/cimon-says-design-lessons-from-a-robot-assistant-in-space/

[¶] https://www.dlr.de/en/research-and-transfer/projects-and-missions/horizons/cimon

[¨] https://www.dlr.de/en/latest/news/2020/02/20200415_cimon-2-makes-its-debut-on-the-iss

sors being used, e.g., with Astrobee and Int-Ball2 using consumer-grade Arm9 processors and running Linux as their operating systems.

The PSA had two processors, a general processing unit (GPU), and a Vision Processing Unit (VPU). The GPU was a Commercial PC104+ card with a 700 MHz Pentium III processor, that ran GNU Linux operating system. The VPU was a custom PC104+ card based on a Xilinx Virtex II Pro FPGA. Operating at 15 Hz, the VPU synchronously performed the capturing and processing of images, along with audio encoding and decoding. Similarly, the SPHERES used two micro-processors, the main software processor being Texas Instruments C6701 DSP which controls the whole unit. The second processor was Tattletale 8 from Onset Technologies', a Motorola 68K processor that dealt with the PADS (state estimation)-related functions. SPHERES code was written in ASCII C.

The SPHERES software ran on asynchronous multi-level interrupts. It had three components, the time-critical controller and propulsion processes, which were interrupt-driven, and a background process that ran all the non time-dependent modules. The propulsion interrupt had the highest priority and ran at 1kHz, and provided interface to the thrusters. Next in the line of priority was the controller interrupt, which ran at 50Hz. This process performed a readout of the metrology data, state estimation and control, and sent the thruster commands to the propulsion interrupt at 10Hz. The other processes contained modules such as housekeeping and communications, which were dubbed as background processes and were not time-dependent, i.e., they ran when neither interrupts were being handled.

In the case of Int-Ball[††], there are three control boards, an Armadillo which runs the complete Int-Ball operation system, the Phenox, a Dual Core ARM9 processor, and an "All-in-one" module. The first two platforms ran LinuxOS while the last ran free-RTOS as a platform. The Phenox board is in charge of image recording and processing, while the All-in-one board conducts high precision state estimation and control. The flight control and measurement cycle runs at 10Hz. [14]. Int-Ball2 most likely runs ROS2 [33].

Astrobee also has a three-processor computing framework [34, 35]: the Low-level processor (LLP) is a Dual Cortex A9 processor running Ubuntu, while the High-level and mid-level processors (HLP and MLP) are Qualcomm SnapDragon running Android and Linux respectively. The robot software is written in C++, has ROS as middleware. The LLP runs high-frequency and timing sensitive tasks such as propulsion, the MLP which runs the computationally intensive flight software, including mobility, fault management, vision-based localization and obstacle detection, and a high-level processor (HLP) which runs the guest science applications and devices for human-robot interaction.

[††]https://www.eoportal.org/other-space-activities/iss-int-ball

3.5 Autonomy modes and requirements of IVFFS

Although the goal is complete free-flyer autonomy, autonomous execution of tasks under high-level command is a stepping stone towards the former. Teleoperation via crew or ground control is still an important capability, especially in the case of Fault Detection And Recovery (FDIR). After analysis of the past and current IVFFS and their capabilities, the following are deemed essential for future IVFFS tasked with the maintenance of orbiting stations:

- Autonomous navigation and position keeping
- Autonomous recharging
- Cargo transportation and handling
- Reactivity to dynamic environments, e.g., replanning and obstacle avoidance
- Appropriate sensors for inventory-keeping and monitoring
- Precise maneuverability in constrained workspaces
- Remote operation, from a ground station or from within the habitat

4. In-space intra-vehicular manipulation

Intra-vehicular manipulation offers significant benefits for future space missions. IVFFS with manipulation capabilities can be used for payload transportation, setting up and managing experiments, as well as housekeeping and maintenance onboard the spacecraft. This not only reduces the crew workload, but will also lead to a potential increase in the amount of experiments and tasks that can be performed without crew intervention. In particular, for uncrewed space stations like the planned Lunar Gateway, intra-vehicular manipulation would be essential to ensure smooth functioning of the station. Out of the IVFFS deployed on the ISS, only Astrobee is equipped with an arm capable of manipulating objects, although it is primarily a perching arm and has not specifically been used for object manipulation and transport.

Robot manipulators on satellites have been studied well in the context of on-orbit manipulation tasks. Multiple robotic arms have been deployed on the ISS, e.g., the Canadarm2 [36], Dextre [37], ERA [38], JEMRMS [39], as well as in the Chinese Space Station, which help in inspection and repairs, docking and on-orbit assembly, and

assisting the crew during EVA. Additionally, robotic arms have been deployed aboard spacecraft, e.g. the ETS-VII mission, the Canadarm on board the Space Shuttle and the arms aboard the Orbital Express that demonstrated the possibility of on-orbit payload manipulation. Multiple robotic on-orbit servicing missions have been planned, where the goal is for a robot manipulator to perform operations such as grasping and berthing, Orbital Replacement Unit (ORU) exchange, repair and maintenance. Some examples of these missions are: EROSS IOD [40], demonstration of the MRV from Northrup Grumman [41]. Generally, when the robotic arms are attached to the top of a large satellite body such as a space station, the effects of free-floating dynamics will be negligible. However, for a free-flying satellite body these effects will be more pronounced. Therefore, the domain of extra-vehicular manipulation has been widely explored in research.

A typical Space Manipulator System consists of a satellite base equipped with one or more robotic arms, and it can be operated in *free-flying* mode, in which the base is actuated through thrusters, or *free-floating* mode, in which the system center of mass cannot translate and the spacecraft translates and rotates in response to manipulator motions due the conservation of momentum; if the attitude of the base is controlled, with reaction wheels for example, the mode is called *partial free-floating*. The coupling dynamics between the manipulator and the base body is the main characteristic of this kind of manipulation, in fact the disturbances due to manipulator motion can become critical and must be accounted for in the motion planning to achieve precise manipulation. Multiple planning and control approaches have been proposed to address dynamic singularities [42], coupling dynamics [43]. With regard to control algorithms, as stated in [44], practically all those used for fixed-base robots can be used for floating-base robots, as the structure of the kinematics and dynamics equations are very similar, the only difference being that the base attitude must be estimated or measured.

Even though these effects also apply to intra-vehicular manipulation, the latter comes with its own challenges. For instance, IVFFS will often have to operate in cluttered and dynamic environments with a limited workspace volume. Therefore, advanced control algorithms that account for the effects of reaction forces will be critical for these operations. Furthermore, there is a possibility that IVFFS will maneuver payloads that are of comparable or larger size than that of the robot base itself. Additionally, the challenges of operating IVFFS are closely linked with the challenges of intra-vehicular cargo handling and transportation. Specifically, localization in intra-vehicular environments needs to be robust to lack of features in the ISS, changing lighting conditions and a dynamic environment. Given the size of the free-flyer and the workspace volume, IVFFS will most likely not use a camera on their arm for visual servoing unlike their orbital counterparts, relying instead on cameras on the robot base. This further emphasizes the need for robust navigation techniques. Other typical challenges for free-flyers comprehend the safety of the crew during operations, navigating the airflow in the ISS to hold position, and deploying planning and control algorithms that consider the coupling effects of multi-body free-flyer dynamics on the limited computing available onboard these miniature satellites.

Free-flying manipulation in indoor micro-gravity environments has been sparsely addressed in literature, with research focusing primarily on the task of grasping itself. For instance, a gecko-inspired adhesive gripper was tested on Astrobee [2]. These kind of grippers allow space robots to grasp and manipulate large items or anchor themselves on smooth surfaces, and they can function in vacuum and withstand extreme temperatures and radiations. Moreover, simulations with an active wrist and adhesive grippers mounted on SPHERES have been run [45], showing that, together with torque control, they increase the range of possible objects that can be manipulated. Astrobee's perching robotic arm has been used for testing orbital hopping maneuvers, [3]. Such maneuvers are of interest in applications like observation, cargo transport and sensor data collection.

4.1 Intra-vehicular Manipulation Simulation Study

Despite the support and dexterity offered by manipulator robots to assist astronauts in routine tasks, intra-vehicular robot manipulation has been scarcely addressed in literature. In the following section, we present initial results from a simulation study for a sample cargo-bag grasping scenario by an IVFFS modeled on NASA's Astrobee free-flyer with a perching arm. The goal is to study the behaviour and nature of free-flyer dynamics, in particular, in floating base systems while carrying out intra-vehicular manipulation.

4.1.1 Simulation scenario

We model our free-flyer based on the Astrobee robot as a cube equipped with a two DoF arm. The links are modeled as cylinders. The dimensions, masses and inertias are presented in Table 2.

The simulation scenario is illustrated in fig. 3. The robot arm starts with the end-effector at position A. In this pose it has zero initial velocities and accelerations, as well as initial momentum. It then approaches the payload at point B by moving joint $q1$ by 60 degrees. The payload is assumed to be stationary, i.e., stowed inside the space

Table 2. Model data

Link	Dimensions (cm)	Mass (kg)	$I_{xx}, I_{yy}, I_{zz} (kg.m^2)$
Base	$32 \times 32 \times 32$	6	0.17, 0.16, 0.19
Link1	$l_1 = 15, r_1 = 2.5$	0.162	3.291e-4, 3.291e-4, 0.253e-4
Link2	$l_1 = 10, r_1 = 2.5$	0.103	1.019e-4 , 1.019e-4 , 0.161e-4

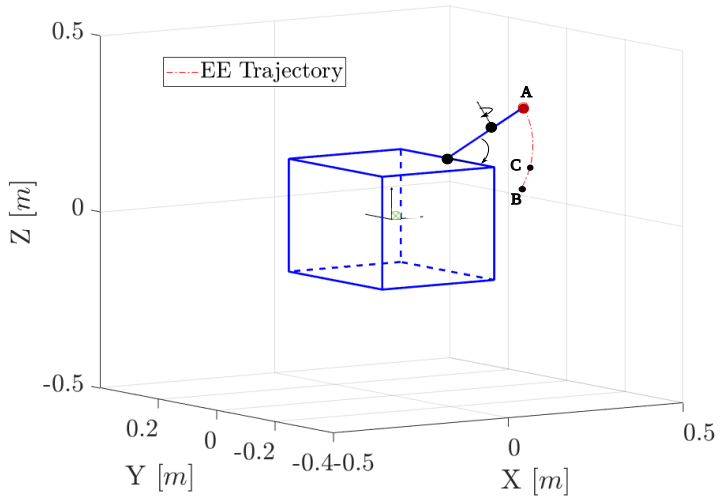

Fig. 3. The robot base and the end-effector used for the simulation of intra-vehicular dynamics. The desired end-effector trajectory A-C is also marked; the payload is grasped at point B.

Table 3. Dimensions and inertial properties of the considered payloads. Length, width and height are denoted by *l*, *w*, and *h*, respectively

Cargo	Mass (kg)	I_{xx}, I_{yy}, I_{zz} (kg.m^2)
CTB0.5 [*l* = 42.5 (cm), *w* = 24.8, *h* = 23.5]		
L1	1	0.0097, 0.0197, 0.0202
L2	2.5	0.0243, 0.0491, 0.0504
L3	5	0.0486, 0.0983, 0.1009
L4	7.3	0.0719, 0.1435, 0.1473
CTB1 [*l* = 42.5 (cm), *w* = 24.8, *h* = 50.2]		
L5	7.3	0.1907, 0.2632, 0.1473
L6	10	0.2613, 0.3605, 0.2018
L7	12.5	0.3266, 0.4507, 0.2522
L8	15.4	0.4023, 0.5552, 0.3107

station. After successful grasping of the payload, the arm moves the payload by moving the first joint in the opposite direction by 15 degrees to reach point C (reconfiguration phase). As an effect of the coupling between the robot base and the arm, and since the commands are sent in open loop, point C for the end-effector will be different depending on the payload.

Given the desired end-effector trajectory $\dot{x}_{ee}$, the joint velocities $\dot{\theta}_m$ are found via the kinematic equation relation of end-effector velocity as

$$\dot{\theta}_m = \hat{J}_m^{-1}(\dot{x}_{ee} - J_b \dot{x}_b) \quad [1]$$

Here, J_m and J_b denotes the manipulator and base Jacobian, respectively, and $\dot{x}_b$ is the base velocity. The base motion is found through the conservation of the system's total momentum.

To observe the dynamics effects of different payloads, we consider payloads with the dimensions of a standard Cargo Transfer Bag (CTB) [‡‡]. We consider two standard

[‡‡] https://go.stratasys.com/rs/533-LAV-099/images/Cargo%20Packing%20Checklist%20-%20Provided%20Data.pdf?version=0

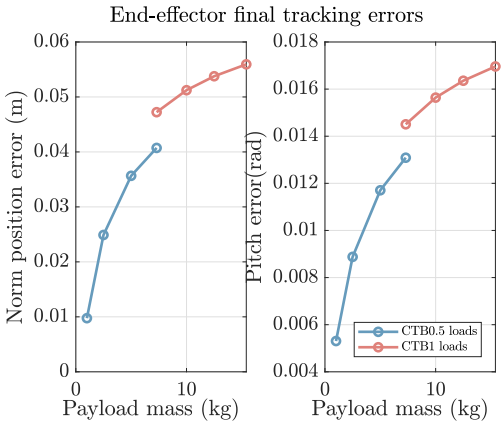

Fig. 4. End-effector tracking errors in free-floating mode

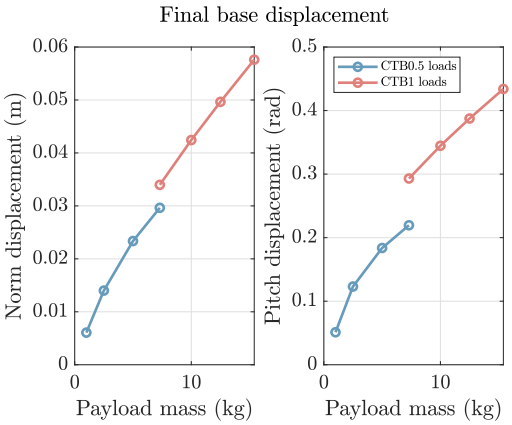

Fig. 5. Base position and pitch displacement in free-floating mode

types of CTBs, CTB0.5 and CTB1, with the dimensions shown in table 3. These bags are considered to have different masses, from partially loaded to fully loaded, with four variations corresponding to each CTB type, i.e., eight cases in total ranging from masses 1 kg to 15.4 kg. Note that the difference in size between the CTB0.5 and CTB1 is only along one dimension. We take that dimension as the payload height, h, so that this change impacts the manipulator's post-grasping movement. Through these variations, we study the effect of increasing payload mass and size (and consequently payload inertia), for such a cargo grasping and reconfiguration task.

In this simulation scenario, limits were imposed on the joint velocities as $0.12\ rad/s$, as stated in the Astrobee URDF[§§]. To determine the feasibility of a manipulation action, we consider the base actuation to be limited at 0.4N for forces and the max applicable torque to be 0.02 Nm.

The free-floating mode is often considered for close proximity operations in orbital robotics. Since only the manipulator arm is controlled in this mode while the base is free to move in response to the robotic arm motion, precise movements can be obtained from the end-effector without disturbance due to base thrusts. On the other hand, in cluttered and dynamic environments, the free-flying mode is preferred to avoid collisions and instability due to the uncontrolled base motion. In the study we consider both scenarios: Performing the cargo-grasping maneuver in 1., free-floating mode, and 2., with the base stabilized.

The trajectories are commanded to the robot in open loop, and for each case, joint torques and base wrenches required for the maneuver, as well as the end-effector tracking errors are studied. This simulation was carried out in Matlab using SPART [¶¶], a modeling and control software package for mobile-base robotic multibody systems, to derive the kinematic and dynamic properties of the system. A few simplifying assumptions were made:

- The robot and the payload are rigid bodies
- A successful grasping is assumed, and the grasping is not modeled
- The payload in the post-grasping phase is modeled as a point mass at the end-effector.

4.1.2 Results

During the **free-floating** manipulation phase, joint q_1 is moved, and the robot arm rotates downwards to approach the payload. The base moves due to the reaction forces and torques transmitted because of the momentum conservation. When the robot grasps the payload and the arm rotates upward, the effects of the base reaction motion increase depending on the mass and inertia of the payload. Figure 6 shows the joint torques required to execute this motion for each of the payloads. The lines in blue show data corresponding to the CTB1 payload, while the red lines correspond to CTB 0.5. Evidently, with increasing payloads, a larger magnitude of joint torques is needed. Further, the change in CTB dimensions also has an impact on the trend, with higher joint torques being required at each step for CTB1 loads. In Figures 4 and 5, the end-effector tracking error at the end of the maneuver and the final base displacement are plotted. The trend here is clear, both these quantities increase with an increase in

[§§] https://github.com/nasa/astrobee/blob/master/description/description/urdf/macro_perching_arm.urdf.xacro

[¶¶] https://github.com/NPS-SRL/SPART

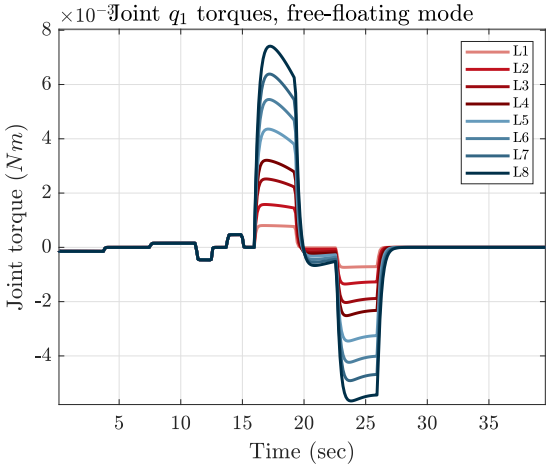

Fig. 6. Joint q_1 torques during the maneuver in free-floating mode. Grasping happens at t=16 secs.

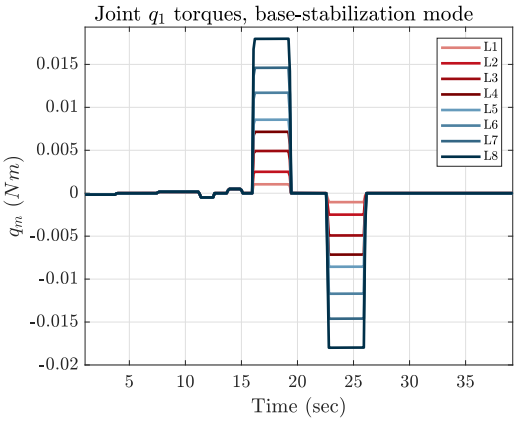

Fig. 7. Joint q_1 torques during the maneuver in base-stabilization mode. Grasping happens at t=16 secs.

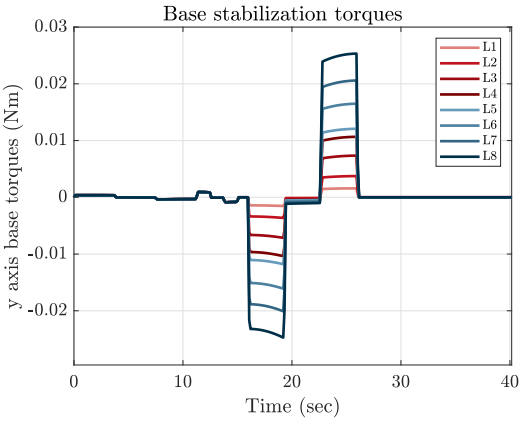

Fig. 8. Base stabilization torques about the Y axis, expressed in the base body frame. Note the violation of the torque limits (>0.2Nm) for higher payloads

mass of the payload. Note that the change in inertia without a change in mass also affects the end-effector position and orientation tracking. However, the base angular displacement is affected more than the linear displacement.

In the **base-stabilization** phase, the same grasping maneuver is carried out, with torques applied to the robot base to keep it still as the joint moves. In this mode, the lack of reaction forces means that the end-effector trajectory tracking improves greatly, with errors for all payloads being 0.9495e-03 m for norm of position errors and 0.0038 rad being the pitch error. At the same time, however, base-stabilization torques are needed for base pose regulation. The y-axis torques are shown in figure 7, which increase as the payload increases. It is important to notice that the maximum thrusts are defined in the local reference system of the base, so they are dependent on its attitude, which is influenced by the manipulator motion in the free-floating phase. Note that this is only base stabilization, which means that moving the robot in free-flying mode, where the base has to be actuated to follow a commanded trajectory with the payload could demand more torques from the system, posing challenges to the transportation of heavier payloads.

Finally, figure 9 shows a 2D view of the final position of the base and the end-effector after the grasping maneuver. It is evident that the reaction forces hinder the end-effector from reaching its final position in the free-floating mode. Manuvering a higher mass would result in these coupling forces becoming difficult to ignore.

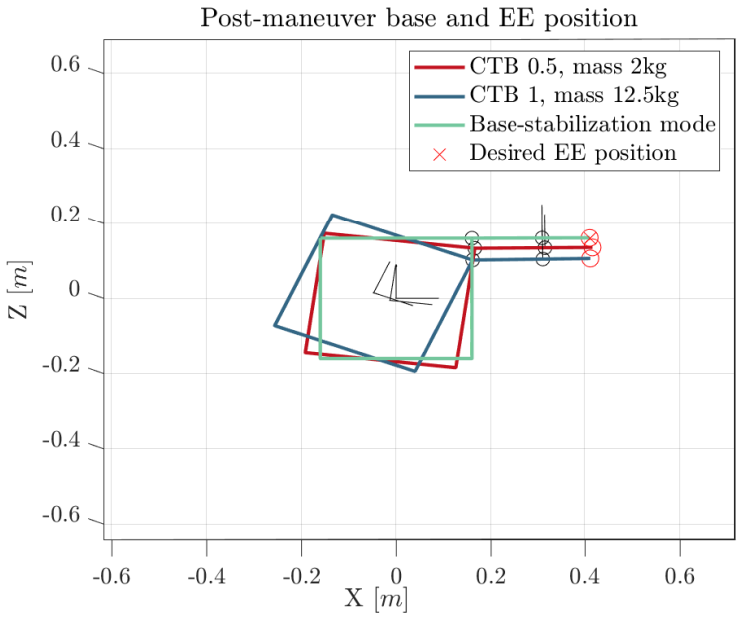

Fig. 9. Planar view of the base and end-effector pose at the end of the grasping maneuver

4.2 Discussion and future work

The analysis above showed the significant effects of the coupling dynamics between the robot body and the manipulator. These effects are most significant in the free-floating mode of operation, where the base is left unactuated for precise motion of the arm without additional disturbances from base actuation. Clearly, feedback control is needed to successfully complete tasks in this mode. Although the base-stabilization mode of operation largely reduced the end-effector error, it required increasingly higher actuation torques to maintain the base position. Irrespective of which mode of operation is used for payload grasping, the free-flying mode is required for cargo transportation. Additionally, as the simulation showed, the robot can carry payloads larger and heavier than itself as long its torque, thrust and motion limits allow, but the payload characteristics influence the robot dynamics and must be accounted for. Therefore, model-based control and planning frameworks with collision avoidance are essential for successful intra-vehicular payload transportation. Future work will continue to focus on studying the coupling dynamics impacting intra-vehicular robot manipulation, in particular, the dynamics of a dual arm robot to perform on-orbit house-keeping tasks.

5. Conclusions

In this paper we presented a survey of existing IVFFS, describing their requirements and features, the challenges that they encountered and the experiments that have been hosted on these platforms. IVFFS have been proposed to perform tasks such as cargo handling and transportation, logistics and equipment swaps to help the crew members and reduce their workloads and, furthermore, accomplish uncrewed space station autonomy for future missions. However, manipulation using IVFFS has scarcely been addressed in literature. Out of the free-flyers deployed in orbit, only Astrobee has a 2 DoF robotic arm, which is primarily intended for perching; therefore, intra-vehicular manipulation using robotic free-flyers has been demonstrated in a limited capacity on-orbit. This paper addresses the subject by discussing the main challenges for intra-vehicular manipulation and presents an analysis that highlights the dynamic coupling effects to be considered when carrying out this task with intra-vehicular free-flyers.

References

[1] S. Yamaguchi, R. Itakura, and T. Inagaki, "ISS/JEM crew-task analysis to support astronauts with intra-vehicular robotics," in *Proc. IEEE Int. Conf. on Robot and Human Interactive Communication (RO-MAN)*, 2023, pp. 1071–1076.

[2] T. G. Chen, A. Cauligi, S. A. Suresh, M. Pavone, and M. R. Cutkosky, "Testing gecko-inspired adhesives with Astrobee aboard the International Space Station: Readying the technology for space," *IEEE Robotics & Automation Magazine*, vol. 29, no. 3, pp. 24–33, 2022.

[3] S. T. Kwok-Choon, M. Romano, and J. Hudson, "Orbital hopping maneuvers with Astrobee onboard the International Space Station," *Acta Astronautica*, vol. 207, pp. 62–76, 2023.

[4] S. Kwok-Choon, J. Hudson, and M. Romano, "Orbital hopping maneuvers with two Astrobee freeflyers: Ground and flight experiments," *Frontiers in Robotics and AI*, vol. 9, p. 1 004 165, 2022.

[5] M. Oda, K. Kibe, and F. Yamagata, "ETS-VII, space robot in-orbit experiment satellite," in *Proc. IEEE Int. Conf. on robotics and automation*, 1996, pp. 739–744.

[6] A. Ogilvie, J. Allport, M. Hannah, and J. Lymer, "Autonomous satellite servicing using the orbital express demonstration manipulator system," in *Proc. Int. Symp. on Artificial Intelligence, Robotics and Automation in Space (i-SAIRAS)*, 2008, pp. 25–29.

[7] K. Nicewarner and G. Dorais, "Designing and validating an adjustably-autonomous free-flying intraspacecraft robot," in *Space*, 2006, p. 7395.

[8] P. L. Swaim, C. J. Thompson, and P. D. Campbell, "The Charlotte (TM) intra-vehicular robot," in *JPL, Int. Symp. on Artificial Intelligence, Robotics, and Automation for Space*, 1994.

[9] S. E. Fredrickson, S. Duran, N. Howard, and J. D. Wagenknecht, "Application of the mini AERCam free flyer for orbital inspection," in *Spacecraft Platforms and Infrastructure*, SPIE, vol. 5419, 2004, pp. 26–35.

[10] S. Fredrickson, S. Duran, A. Braun, T. Straube, and J. Mitchell, "AERCam autonomy: Intelligent software architecture for robotic free flying nanosatellite inspection vehicles," in *Space*, 2006, p. 7392.

[11] S. E. Fredrickson, "Mini AERCam for in-space inspection," in *In-Space Non-Destructive Inspection Technology Meeting*, 2012.

[12] G. A. Dorais and Y. Gawdiak, "The Personal Satellite Assistant: An internal spacecraft autonomous mobile monitor," in *Proc. IEEE Aerospace Conf.*, vol. 1, 2003, pp. 1–348.

[13] N. Smith, D. Peters, C. Jay, G. M. Sandal, E. C. Barrett, R. Wuebker, *et al.*, "Off-world mental health: Considerations for the design of well-being–supportive technologies for deep space exploration," *JMIR Formative Research*, vol. 7, no. 1, e37784, 2023.

[14] S. Mitani *et al.*, "Int-ball: Crew-supportive autonomous mobile camera robot on ISS/JEM," in *Proc. IEEE Aerospace Conf.*, 2019, pp. 1–15.

[15] T. Nishishita *et al.*, "Complementary ground testing method for autonomous flight system of space free-flying robot," in *Proc. IEEE Aerospace Conf.*, 2024, pp. 1–12.

[16] A. S. Otero, A. Chen, D. W. Miller, and M. Hilstad, "SPHERES: Development of an ISS laboratory for formation flight and docking research," in *Proc. IEEE Aerospace Conf.*, 2002.

[17] J. Enright, M. Hilstad, A. Saenz-Otero, and D. Miller, "The SPHERES guest scientist program: Collaborative science on the ISS," in *Proc. IEEE Aerospace Conf.*, vol. 1, 2004.

[18] S. Nolet and D. W. Miller, "Autonomous docking experiments using the SPHERES testbed inside the ISS," in *Sensors and Systems for Space Applications*, Int. Society for Optics and Photonics, vol. 6555, SPIE, 2007.

[19] G. Lapilli *et al.*, "Results of microgravity fluid dynamics captured with the SPHERES-slosh experiment," in *Proc. Int. Astronautical Congress*, 2015.

[20] A. Porter *et al.*, "Demonstration of electromagnetic formation flight and wireless power transfer," *J. of Spacecraft and Rockets*, vol. 51, no. 6, pp. 1914–1923, 2014.

[21] M. G. Bualat, T. Smith, E. E. Smith, T. Fong, and D. Wheeler, "Astrobee: A new tool for ISS operations," in *Proc. SpaceOps Conf.*, 2018, p. 2517.

[22] M. K. Mckinley, "Logistics reduction: RFID enabled autonomous logistics management (REALM) (LR-REALM)," *NASA TechPort*, 2021.

[23] K. Albee *et al.*, "Autonomous rendezvous with an uncertain, uncooperative tumbling target: The Tumbledock flight experiments," in *Proc. Symp. on Advanced Space Technologies in Robotics and Automation (ASTRA)*, 2022.

[24] B. Doerr, K. Albee, M. Ekal, R. Ventura, and R. Linares, "The ReSWARM microgravity flight experiments: Planning, control, and model estimation for on-orbit close proximity operations," *J. of Field Robotics*, vol. 41, no. 6, pp. 1645–1679, 2023.

[25] Y. Tsumaki and I. Maeda, "Intra-vehicular freeflyer with manipulation capability," *Advanced Robotics*, vol. 24, no. 3, pp. 343–358, 2010.

[26] R. Ventura, P. Roque, and M. Ekal, "Towards an autonomous free-flying robot fleet for intra-vehicular transportation of loads in unmanned space stations," in *Proc. Int. Astronautical Congress (IAC)*, 2018.

[27] P. D. Campbell, P. L. Swaim, and C. J. Thompson, "Charlotte™ robot technology for space and terrestrial applications," *SAE Transactions*, pp. 641–648, 1995.

[28] R. Soussan, V. Kumar, B. Coltin, and T. Smith, "Astroloc: An efficient and robust localizer for a free-flying robot," in *Proc. Int. Conf. on Robotics and Automation (ICRA)*, 2022, pp. 4106–4112.

[29] E. Daley, "Astrobee free-flyer nozzle mechanism," in *Proc. Aerospace Mechanism Symp.*, 2020.

[30] V. Schröder, R. Regele, J. Sommer, T. Eisenberg, and C. Karrasch, "GNC system design for the crew interactive mobile companion (CIMON)," in *Proc. IAF Human Spaceflight Symposium at Int. Astronautical Congress (IAC)*, 2018.

[31] T. Nishishita *et al.*, "Complementary ground testing method for autonomous flight system of space free-flying robot," in *Proc. IEEE Aerospace Conf.*, 2024, pp. 1–12.

[32] T. Smith *et al.*, "Astrobee: A new platform for free-flying robotics on the International Space Station," in *Proc. Int. Symp. on Artificial Intelligence, Robotics, and Automation in Space (i-SAIRAS)*, 2016.

[33] H. Kato and T. Saito, "RACS2: the ROS2 and cFS system, launched," in *Flight Software Workshop*, JAXA and Systems Engineering Consultants (SEC), Mar. 2023.

[34] J. Yoo, I.-W. Park, V. To, J. Q. Lum, and T. Smith, "Avionics and perching systems of free-flying robots for the International Space Station," in *Proc. IEEE Int. Symp. on Systems Engineering (ISSE)*, 2015, pp. 198–201.

[35] L. Fluckiger, K. Browne, B. Coltin, J. Fusco, T. Morse, and A. Symington, "Astrobee robot software: A modern software system for space," in *Proc. Int. Symp. on Artificial Intelligence, Robotics and Automation in Space (iSAIRAS)*, 2018.

[36] P. K. Nguyen and M. Hiltz, "RMS operations support: From the space shuttle to the space station," in *Proc. Int. Symp. on Artificial Intelligence and Robotics & Automation in Space (i-SAIRAS)*, 2001, pp. 1–8.

[37] E. Coleshill, L. Oshinowo, R. Rembala, B. Bina, D. Rey, and S. Sindelar, "Dextre: Improving maintenance operations on the international space station," *Acta Astronautica*, vol. 64, no. 9-10, pp. 869–874, 2009.

[38] A. Oort, F. M. Meiboom, and C. J. M. Heemskerk, "How to build a space robot; lessons learned from the european robotic arm program," in *Proce. ESA Workshop on Advanced Space Technologies for Robotics and Automation (ASTRA)*, 2000.

[39] H. Ueno, S. Doi, and H. Morimoto, "Jemrms initial checkout and payload berthing," in *Proc. Int. Symp. on Artificial Intelligence and Robotics & Automation in Space (i-SAIRAS)*, 2010, pp. 867–872.

[40] M. A. Roa *et al.*, "EROSS: In-Orbit Demonstration of European Robotic Orbital Support Services," in *IEEE Aerospace Conf.*, 2024, pp. 1–9.

[41] M. Pyrak and J. Anderson, "Performance of Northrop Grumman's Mission Extension Vehicle (MEV) RPO imagers at GEO," in *Autonomous Systems: Sensors, Processing and Security for Ground, Air, Sea and Space Vehicles and Infrastructure*, M. Dudzik, S. Jameson, and T. Axenson, Eds., vol. 12115, SPIE, 2022, 121150A.

[42] K. Nanos and E. Papadopoulos, "On cartesian motions with singularities avoidance for free-floating space robots," in *Proc. IEEE Int. Conf. on Robotics and Automation (ICRA)*, 2012, pp. 5398–5403.

[43] R. Lampariello, S. Agrawal, and G. Hirzinger, "Optimal motion planning for free-flying robots," in *Proc. IEEE Int. Conf. on Robotics and Automation (ICRA)*, vol. 3, 2003, pp. 3029–3035.

[44] E. Papadopoulos and S. Dubowsky, "On the nature of control algorithms for free-floating space manipulators," *IEEE Trans. on Robotics and Automation*, vol. 7, no. 6, pp. 750–758, 1991.

[45] M. A. Estrada, H. Jiang, B. Noll, E. W. Hawkes, M. Pavone, and M. R. Cutkosky, "Force and moment constraints of a curved surface gripper and wrist for assistive free flyers," in *Proc. IEEE Int. Conf. on Robotics and Automation (ICRA)*, 2017, pp. 2824–2830.